Molecules and Cells

Upregulation of FZD5 in Eosinophilic Chronic Rhinosinusitis with Nasal Polyps by Epigenetic Modification

Jong-Yeup Kim[1,2,*], Min-Ji Cha[1,2], Young-Seon Park[1,2], Jaeku Kang[3,4], Jong-Joong Choi[1], Seung Min In[1], and Dong-Kyu Kim[5,6]

[1]Department of Otorhinolaryngology-Head and Neck Surgery, [2]Department of Biomedical Informatics, [3]Myunggok Medical Research Institute, [4]Department of Pharmacology, College of Medicine, Konyang University, Daejeon 35365, Korea, [5]Department of Otorhinolaryngology-Head and Neck Surgery, Chuncheon Sacred Heart Hospital, [6]Institute of New Frontier Research, Hallym University College of Medicine, Chuncheon 24253, Korea
*Correspondence: k@kyuh.ac.kr
http://dx.doi.org/10.14348/molcells.2019.2418
www.molcells.org

Eosinophilic chronic rhinosinusitis with nasal polyps (CRSwNP) is one of the most challenging problems in clinical rhinology. FZD5 is a receptor for Wnt5A, and its complex with Wnt5A contributes to activating inflammation and tissue modification. Nasal polyps and eosinophil/non-eosinophil counts are reported to be directly correlated. This study investigated the expression and distribution of FZD5, and the role of eosinophil infiltration and FZD5 in eosinophilic CRSwNP pathogenesis. The prognostic role of eosinophil levels was evaluated in seven patients with CRSwNP. Fifteen patients with CRS were classified based on the percentage of eosinophils in nasal polyp tissue. Methylated genes were detected using methyl-CpG-binding domain sequencing, and qRT-PCR and immunohistochemistry were used to detect FZD5 expression in nasal polyp tissue samples. The results showed that mRNA expression of FZD5 was upregulated in nasal polyps. FZD5 expression was significantly higher in nasal polyp samples from patients with eosinophilic CRSwNP than in those from patients with non-eosinophilic CRSwNP, as indicated by immunohistochemistry. Furthermore, inflammatory cytokine levels were higher in eosinophilic CRSwNP-derived epithelial cells than in normal tissues. In conclusion, FZD5 expression in nasal mucosal epithelial cells is correlated with inflammatory cells and might play a role in the pathogenesis of eosinophilic CRSwNP.

Keywords: chronic rhinosinusitis, eosinophils, nasal polyp, nasal polyposis, sinusitis

INTRODUCTION

Chronic rhinosinusitis with nasal polyps (CRSwNP), one of the most prevalent chronic illnesses, affects 4-10% of the global population (Fokkens et al., 2012; Hamilos, 2007; Hsu and Peters, 2011; Sreeparvathi et al., 2017). CRSwNP is characterized by chronic inflammation of the nasal mucosa and paranasal sinuses that persists for a minimum of 12 weeks (Hamilos, 2007; Hsu and Peters, 2011; Sreeparvathi et al., 2017). Based on whether the prevalence of eosinophil tissue infiltration in NP exceeds 10% of the total inflammatory cells, two subtypes can be distinguished: eosinophilic and non-eosinophilic CRSwNP (E-CRSwNP and NE-CRSwNP, respectively)(Grgić et al., 2015; Sreeparvathi et al., 2017). E-CRSwNP is characterized by high eosinophilic infiltration in the polyps, which predicts higher risk for polyp recurrence

Received 31 October, 2018; revised 20 February, 2019; accepted 25 February, 2019; published online 2 April, 2019

eISSN: 0219-1032

after surgical treatment and poor prognosis (Akdis et al., 2013; Payne et al., 2011). A direct correlation between NP and eosinophil/neutrophil counts has been reported (Kim et al., 2015; Shah et al., 2016). Considering the involvement of severe eosinophilic inflammation in E-CRSwNP, there is a need for more aggressive treatments and surgical therapies (Derycke et al., 2014). While various studies have been conducted to clarify the different cellular and molecular characteristics of chronic inflammation in E-CRSwNP and NE-CRSwNP, the molecular mechanisms underlying the differences remain largely unknown (Chen et al., 2018, Chin and Harvey, 2013).

Eosinophils are bone marrow-derived leukocytes normally present in low numbers in the blood (typically < 5% of all white blood cells)(Ponikau et al., 2003; Yao et al., 2013). However, in pathological states, eosinophils are rapidly activated and then migrate to the site of injury where they release mediators, including cytokines, chemokines, and cytotoxic granule proteins, such as eosinophilic cationic protein, eosinophilic peroxidase, and major basic protein (Busche et al., 2015; Doran et al., 2007; Rothenberg, 1998; 2001; Rothenberg and Hogan, 2006). The increase in eosinophil numbers and, consequently, interleukin (IL)-4, -5, and -13, is associated with type 2 inflammation (Busche et al., 2015; Lin et al., 2007; Rothenberg et al., 2001). Multiple types of inflammatory mediators have been shown to be upregulated in the inflammatory mucosa of E-CRSwNP. However, the precise mechanism of the pathogenesis of E-CRSwNP remains unclear and, therefore, we sought to elucidate the mechanism using epigenetics.

Wnt proteins form a very large family of secreted ligands that activate several receptor-mediated signal transduction pathways (Lin et al., 2007; Ueno et al., 2007). In the canonical Wnt signaling pathway, binding of Wnt to the frizzled family receptor (FZD) class of transmembrane receptors inhibits a protein complex responsible for the degradation of the cytosolic effector (Ueno et al., 2007). FZD is a family of G protein-coupled receptors that function in the Wnt and other signaling pathways (Malbon, 2004; Peterson et al., 2017; Rothenberg, 1998). FZD proteins are receptors for secreted Wnt proteins and other ligands (Ingham and McMahon, 2001; Rothenberg, 1998; Rothenberg and Hogan, 2006). Following stimulation, FZD activates canonical and non-canonical Wnt signaling pathways in the cytosol (Huang and Klein, 2004). Thus, its biologically active form plays a role as an endogenous danger signal (Malbon, 2004). It is not yet clear how FZD proteins couple to downstream effectors in E-CRSwNP.

Epigenetics has recently been proposed as an explanation for the key genetic/environmental interactions involved in NP formation (Fokkens et al., 2012; Ingham and McMahon, 2001). The mechanisms of epigenetic regulation underlie many complex diseases and, therefore, might contribute to the development and heritability of paranasal disease (North and Ellis, 2011). The review by North and Ellis (2011) highlighted the importance of epigenetic modifications in the developmental origins and pathogenesis of asthma and other atopic diseases, suggesting a potential for future application of epigenetic targets to the clinical management of allergy and immunology. Thus, a better understanding of the role of DNA methylation in NP formation is required to inform focused epigenetic studies toward the realization of clinical applications.

In a previous study, we showed that methylation levels are changed in NP (Kim et al., 2018). In this study, we aimed to compare methylation in E-CRSwNP with that in NE-CRSwNP and to identify the significance of FZD5 in E-CRSwNP. Methylated genes were detected using methyl-CpG-binding domain sequencing (MBD-seq) and validated using methylation-specific polymerase chain reaction (PCR), bisulfite sequencing, and real-time PCR. To identify genes that are differentially methylated in E-CRSwNP, we compared the methylation profile of E-CRSwNP to the control profile. Further, we examined the prognostic value of eosinophil and neutrophil levels in NP tissues in patients with bilateral NP. Identifying the mechanism of E-CRSwNP development may reveal crucial information for clinical treatment.

MATERIALS AND METHODS

Ethics statement

This study was based on data acquired from the Konyang University Hospital through a survey conducted by the Center for Otorhinolaryngology. The protocol was approved by the Institutional Review Board of Konyang University Hospital (approval no. 2017-12-014), and all subjects provided written informed consent prior to inclusion in the study. All experiments were carried out in accordance with the relevant guidelines and regulations.

Subjects and sample collection

The diagnosis of CRS was based on the definition of the European Position Paper on Rhinosinusitis and Nasal Polyps 2012 (Chin and Harvey, 2013). In total, 23 subjects were included in the study, and they were divided into three groups: E-CRSwNP (n = 7), NE-CRSwNP (n = 8), and controls (n = 8 each). Patients selected for the control group had undergone endoscopic transsphenoidal surgery for CRSwNP and had an average age of 47.5 years. Patients with CRSwNP ranged in age from 18 to 76 years (average, 48.29 years). All seven patients with CRSwNP underwent revision sinus surgery. All patients were non-smokers. In this study, we obtained uncinate process (UP) mucosa tissues from control subjects and inflamed UP tissues from the patients with CRS, including those of the chronic rhinosinusitis without nasal polyps (CRSsNP) and CRSwNP groups. We also evaluated NP tissues, obtained during surgery, from patients with CRSwNP (Table 1).

The exclusion criteria were as follows: (1) abnormal atopic status (eosinophil count outside of the normal range and increased immunoCAP IgE levels); (2) history of smoking; (3) prior treatment with oral or spray steroids for three months before surgery; and (4) cystic fibrosis, congenital mucociliary problems, systemic vasculitis, gastroesophageal reflux diseases, antrochoanal polyp, and fungal sinusitis. Controls with allergic rhinitis were also excluded. Each tissue sample was divided into two parts: one part was fixed in 10% formaldehyde and embedded in paraffin for histological analysis, and the

Table 1. Clinical characteristics of patients included in this study

Characteristics	Control	CRSwNP	
		eosinophilic	non-eosinophilic
Subjects (no.)	8	7	8
Gender (M/F)	4/4	5/2	6/2
Age (y)	47.5 ± 15.35	46.9 ± 12.52	49.7 ± 22.74
Allergic rhinitis, N	0	0	0
Aspirin sensitivity, N	0	0	0
Lund-Mackay CT score	4.13 ± 3.78	11.00 ± 4.90	7.50 ± 4.26
Lund-Kennedy score	4.38 ± 2.23	8.71 ± 1.90	6.63 ± 2.04
Polyp characteristics	n/a	eosinophilic	non-eosinophilic
Methodologies used			
DNA methylation	8	6	5
Tissue IHC	8	7	8
qRT-PCR	3	3	3
Western blot	3	3	3

other was immediately snap-frozen in liquid nitrogen and stored at -80℃ for RNA, DNA, and protein extraction. Fresh tissue specimens were quickly cleaned with 0.9% normal saline and sliced into appropriate sections.

HiSeq MBD-seq library preparation

Genomic DNA was isolated from the tissues using a Maxwell® 16 MDx Instrument (Promega, USA) according to the manufacturer's protocols and with settings for tissue DNA. One microgram of genomic DNA was sheared into 200-400-bp fragments using a Covaris LE220 sonicator (Covaris, USA). The fragmented products were immunoprecipitated using a MethylMiner methylated DNA enrichment kit (Invitrogen, USA) according to the manufacturer's protocol. In brief, methylated DNA was isolated from fragmented whole genomic DNA by binding to the MBD of human MBD2 protein, which was coupled to paramagnetic streptavidin beads (Dynabeads® M-280) via a biotin linker. The methylated fragments were eluted as a single enriched population with a 2000 mM sodium chloride (NaCl) elution buffer. The methylated double-stranded DNA was end-repaired, i.e., an "A" was ligated to the 3′ end, and then, Illumina adapters were ligated to the fragments with a target size of 300-500-bp products. The size-selected product was PCR-amplified, and the final product was validated using an Agilent Bioanalyzer (Agilent, USA).

Clustering and sequencing

To explore the molecular basis of the difference between CRSwNP and CRSsNP, we analyzed a flow cell containing millions of unique clusters loaded onto the HiSeq 2000 system for automated cycles of extension and imaging. The Illumina system utilizes a unique "bridged" amplification reaction that occurs on the surface of a flow cell. Illumina's sequencing-by-synthesis system utilizes four proprietary nucleotides possessing reversible fluorophore and termination properties. Each sequencing cycle occurs in the presence of all four nucleotides, leading to higher accuracy than methods involving only one nucleotide in the reaction mixture at a time. The cycle is repeated, one base at a time, generating a series of images, each representing a single base extension at a specific cluster. Raw data of the DNA methylation patterns of the target genes were extracted as paired files using Illumina software.

Data processing and methylation profile calling

Paired-end sequencing reads (100 bp) generated by MBD-seq were verified for sequence quality using FastQC (version 0.10.0). Before starting the analysis, Trimmomatic (version 0.32) was used to remove adapter sequences and bases with a quality score <3 from the read ends. In addition, bases that did not meet the criteria of a window size of 4 and mean quality score of 15 were removed using a sliding-window trim method. Then, reads with a minimum length of 36 bp were removed to produce clean data. The cleaned reads were aligned to the human genome (UCSC hg19) using Bowtie (version 1.1.1, parameter set -n 2-m 1-X500) allowing for up to two nucleotide mismatches to the reference genome per seed and returning only uniquely mapped reads. Mapped data (SAM file format) were subjected to sorting and indexing using SAMtools (version 0.1.19). PCR duplicates were removed using Picard Mark Duplicates (version 1.118). The MBD data were analyzed using the MEDIPS package. For each sample, the aligned reads were extended in the sequencing direction to a length of 300 nt. The sequencing read coverage of the extended reads was calculated at a genome-wide 250-bp window size. Then, the coverage profiles (read count, RPKM, RMS) at each genomic bin were calculated. Each differentially methylated region (DMR) was annotated using the table browser function of the UCSC genome browser. The annotation included gene structures, transcripts, promoter regions (defined as -2 kb upstream of the transcription start site), exons, introns, and CpG islands.

Identification of DMRs

Read counts at each genomic bin were normalized to the

trimmed mean of M-values normalized in the edgeR package. We applied an exact test to assess the significance of the methylation differences between comparison groups using edgeR. DMRs were determined by filtering each region associated with a |log2FC| value ≥1 and exact test *P*-values <0.05.

Hierarchical clustering analysis was conducted using complete linkage and Euclidean distance as a measure of similarity to display the methylation patterns of DMRs that satisfied the significance criteria above for at least one more comparison pair. Gene enrichment and functional annotation analyses were conducted using the Database for Annotation, Visualization, and Integrated Discovery (DAVID) tool (http://david.abcc.ncifcrf.gov/home.jsp). Data analysis and visualization of DMRs were conducted using R 3.0.2 (www.r-project.org).

Quantitative reverse transcription (qRT)-PCR

Total RNA was isolated from nasal tissues with TRIzol reagent (Ambion), according to the manufacturer's instructions. cDNA was synthesized using MMLV reverse transcriptase (Promega). qRT-PCRs were run in triplicate using iQTM SYBR Green Supermix and a CFX96 qPCR instrument (BioRad, USA). Primers are listed in Table 2. Some primers were purchased from Life Technologies Corporation (USA). The amplification conditions were as follows: predenaturation at 95℃ for 3 min, followed by 40 cycles of denaturation at 95℃ for 10 s, annealing at 58℃ for 10 s, and extension at 72℃ for 10 s. The cycle threshold (Ct) comparison method $2^{-\Delta\Delta Ct}$ was used for calculating the relative expression levels, using glyceraldehyde-3-phosphate dehydrogenase (*GAPDH*) as the reference gene.

Western blotting

Protein was extracted from nasal mucosa samples homogenized in lysis buffer (Cell Signaling Technology, USA) with a protease inhibitor and phosphatase inhibitor cocktail (both Roche, Switzerland) at 4℃ for 25 min. Lysates were centrifuged at 16 000 × *g* for 10 min at 4℃. The protein concentrations were determined using a BCA assay (Pierce Biotechnology, USA). Equal amounts of protein were subjected to 10-12% sodium dodecyl sulfate-polyacrylamide gel electrophoresis. Proteins were transferred to polyvinylidene difluoride membranes (Millipore, USA) at 100 V and 135 mA for 100 min. The membranes were blocked with Tris-buffered saline plus 0.1% Tween-20 (TBS-T, both Sigma-Aldrich) and 10% skim milk (BD Biosciences, USA) for 1 h at 25℃ or overnight at 4℃. The blots were then incubated with primary antibodies for 1 h at room temperature or overnight at 4℃. All antibodies were diluted 1:1000 with TBS-T and 5% non-fat dried milk. The membranes were then washed three times in 1× TBS-T at room temperature and incubated with a horseradish peroxidase-conjugated rabbit secondary antibody (Santa Cruz Biotechnology). After washing the membrane six times, immunoreactive proteins were detected using an enhanced chemiluminescence (ECL) system (Amersham Biosciences, Japan). Band intensities were quantified using the ImageJ software (National Institutes of Health [NIH], USA).

Epithelial cell isolation from patient tissues

NP and ethmoid sinus tissue samples of patients with CRSwNP and CRSsNP, respectively, were obtained during surgery. The samples were immediately placed in Dulbecco's modified Eagle's medium (DMEM, Lonza, Switzerland) without serum, supplemented with penicillin 100 U/mL, streptomycin 100 μg/mL, and glutamine. The samples were washed twice in NaCl solution and cut into small pieces (~1 mm^2). Primary nasal epithelial cells were obtained by digesting nasal turbinates or polyps with 0.5 mg/mL collagenase IV (Worthington Biochemical, USA) in phosphate-buffered saline for 1 h. Diced specimens were then plated (density, nine pieces/six-well tissue-culture dish) in DMEM and incubated in a humidified 5% CO_2 atmosphere at 37℃, until a confluent monolayer of epithelial-like cells was observed, usually after 13 ± 2 days. Then, the explanted tissues were trypsinized, and the cells were replated into a six-well tissue culture dish in 1.5 mL of fresh DMEM. The medium was changed every 3 days for 2-3 weeks until 90% confluence was achieved, usually after 17 ± 3 days, when the cells were stimulated overnight.

Table 2. List of primers utilized for qRT-PCR

Genes	Official full name	Catalog number or primer sequences
GAPDH	glyceraldehyde-3-phosphate dehydrogenase	Hs03929097_g1
CDH8	cadherin 8, type 2	Hs00242416_m1
FZD5	frizzled family receptor 5	Hs00258278_s1
GSTT1	glutathione S-transferase theta 1	Hs02512069_s1
PDE4B	phosphodiesterase 4B, cAMP-specific	Hs00277080_m1
WNT2	wingless-type MMTV integration site family member 2	Hs00608224_m1
CCNG1	Cyclin G1	F: GCGAAGCATCTTGGGTGTGT
		R: TCCTTTCCTCTTCAGTCGCTTT
SLC4A8	solute carrier family 4 member 8	F: GCTCAAGAAAGGCTGTGGCTAC
		R: CATGAAGACTGAGCAGCCCATC
RPL17	ribosomal protein L17	F: ACCAGTGCGTCCCCTTCA
		R: CTCATCTTCGGAGCCTTGTTC

Cell proliferation assay

Human nasal epithelial cell (HNEC) viability was determined using a water-soluble tetrazolium 8 [WST-8, 2-(2-methoxy-4-nitrophenyl)-3-(4-nitrophenyl)-5-(2,4-disulfophenyl)-2H-tetrazolium] assay with the cell counting kit (CCK)-8 assay kit (Dojindo, Japan). Epithelial cells were plated in triplicate wells of a 96-well plate at 5×10^3 cells/well. The cells were treated with recombinant human/mouse Wnt-5a (R&D Systems, USA) for 24, 48, or 72 h. Then, the cells were washed twice with medium, and 100 µL CCK-8 reagent was added to each well. The samples were subsequently incubated for 2 h at 37℃. The absorbance in each well was measured at 450 nm against a background control using a microplate reader (Bio-Rad, USA).

Cytokine array

Cytokine array analysis was conducted using the human cytokine array kit (ARY005; R&D Systems) following the manufacturer's instructions. The intensity of the selected dots was analyzed using ImageJ software. Duplicates were averaged, and the background was subtracted to calculate the mean pixel density for each factor.

Histological analysis

Tissue inflammation was characterized by hematoxylin and eosin (H&E) staining, which allowed determination of overall inflammation and the eosinophil-to-non-eosinophil ratio in the subepithelial layer. Surgically procured tissue specimens obtained from the CRSwNP and control groups were formalin-fixed and paraffin-embedded. Paraffin sections (4 µm thick) were stained with H&E according to the manufacturer's instructions. Eosinophils and neutrophils were counted. All parameters were assessed using an image analyzer (SP 500; Olympus, Japan). In total, five randomly selected fields of view were evaluated for each section at a magnification of 400× by two experienced pathologists.

Statistical analysis

Statistical analysis was conducted using the MEDIPS (1.16.0) software package. Methylation data analysis and visualization of DMRs were conducted using R 3.0.2 (www.r-project.org). qRT-PCR data are presented as means ± standard deviations. All results were analyzed using Student's *t*-test, and $P < 0.05$ or $P < 0.01$ was considered statistically significant.

RESULTS

Patient characteristics

The study group consisted of 15 male and 8 female patients with a median age of 51 years (range, 18-76 years). The patients were classified as E-CRSwNP or NE-CRSwNP by eosinophil intensity in polyp tissue. The two subgroups did not significantly differ in age and gender. A comparison of the following risk factors of the two groups (asthma, aspirin sensitivity, smoking, and presence of any systemic disease) revealed no significant differences (Table 1). All patients were nonsmokers. To explore the possible pathogenic mechanisms of different NP types, we divided polyps into three subgroups: control, NE-CRSwNP, and E-CRSwNP (Fig. 1). E-CRSwNP was classified as eosinophilic when the percentage of tissue eosinophils exceeded 10% of the total infiltrating cells.

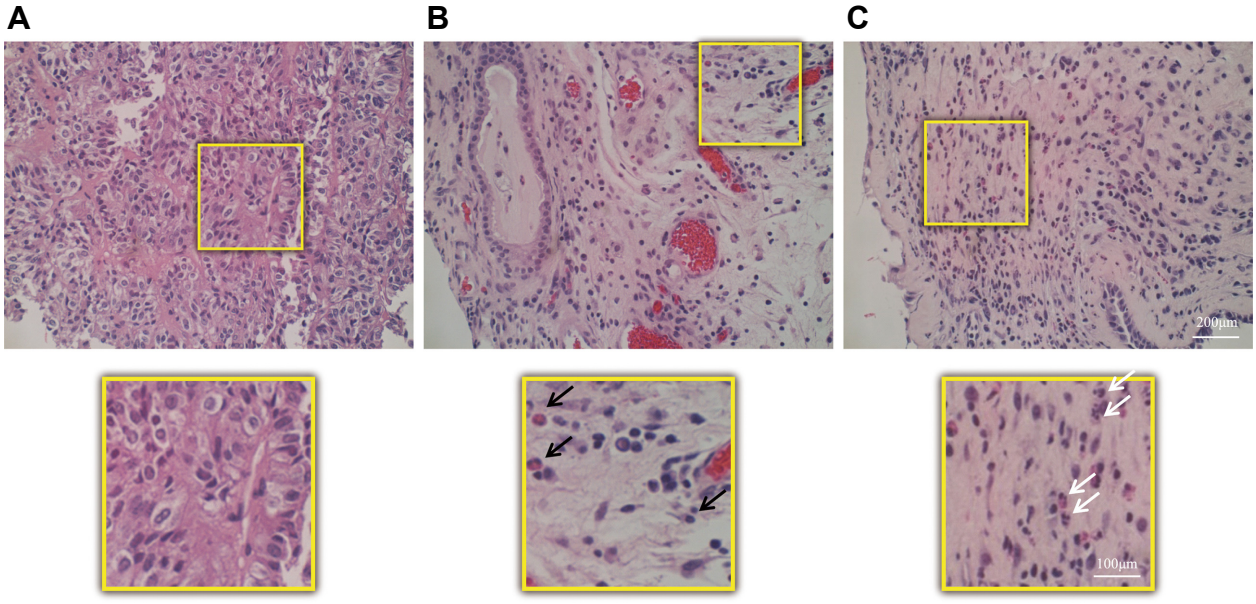

Fig. 1. Immunohistochemical detection of innate immune cells using hematoxylin and eosin (H&E). (A) Control tissue, (B) NP tissue from patients with NE-CRSwNP, (C) NP tissue from patients with E-CRSwNP. Black arrows indicate neutrophilic cells and white arrows indicate eosinophilic cells (magnification, 200×).

MBD-seq analysis

Epigenetic biomarker development, which requires robust discrimination between cell types or disease states, is an important application of DNA methylation assays. DNA methylation profiling based on unsupervised hierarchical clustering identified four unique clusters with distinct methylation signatures (Fig. 2A). We observed a good separation between the different cell types (eosinophils/non-eosinophils) based on methylation changes in E-CRSwNP/NE-CRSwNP versus control (Figs. 2B and 2C). To identify genes that are differentially methylated in E-CRSwNP, we compared the methylation profiles of E-CRSwNP to those of NE-CRSwNP and the control. In total, 397 and 387 genes were differentially hypermethylated in the E-CRSwNP and NE-CRSwNP groups (Fig. 2B), respectively, compared to the control tissues. Furthermore, 399 and 208 genes were hypomethylated in the E-CRSwNP and NE-CRSwNP (Fig. 2C), respectively, compared to control tissues. Four genes exhibited hypermethylation in E-CRSwNP compared to NE-CRSwNP, and 19 genes exhibited hypomethylation in E-CRSwNP compared to NE-CRSwNP (Fig. 2D). We selected the most strongly hypomethylated genes in E-CRSWNP (cadherin 8, type 2 [*CDH8*], *FZD5*, phosphodiesterase 4B, cAMP-specific [*PDE4B*], and *WNT2*).

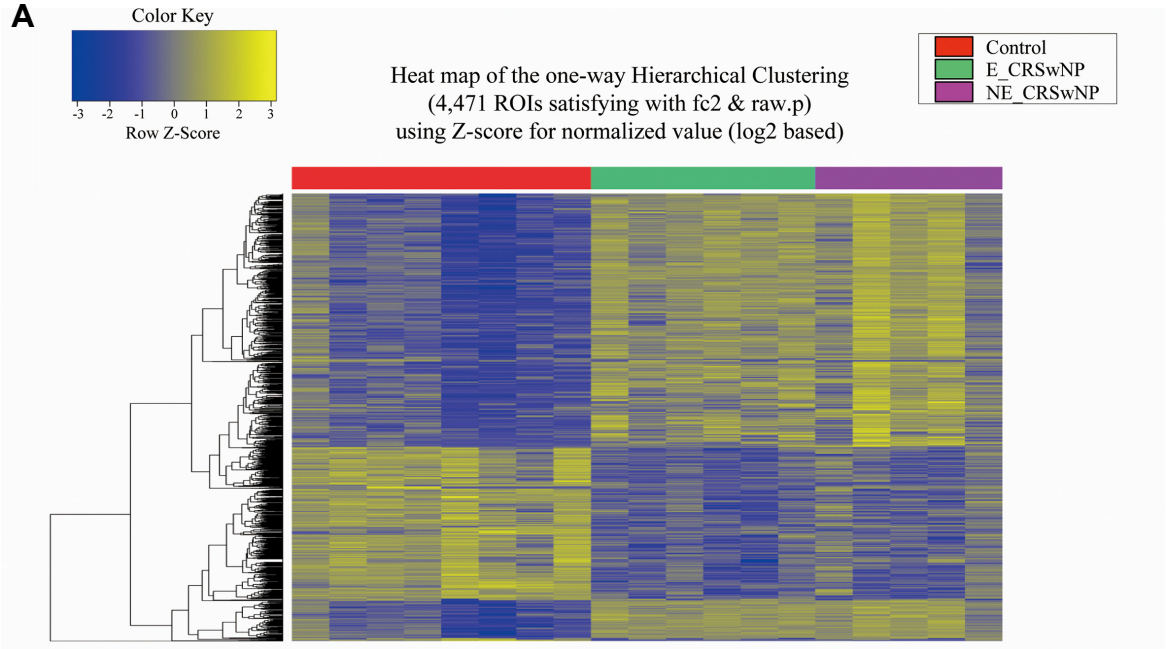

D

E - CRSwNP vs. NE - CRSwNP

Hypermethylation	Hypomethylation		
GSTT1	OPRK1	TARS	DPYSL5
CCNG1	NRP1	FKBP2	**PDE4B**
SLC4A8	**FZD5**	C15orf38 - AP3S2	GSN
RPL17	**CDH8**	PPP3CA	CLASP1
	LMCD1	TRDMT1	KCNC3
	TSTA3	TMEM237	ISPD
			WNT2

Fig. 2. Clustering of samples based on DNA methylation profiles, which identified four unique clusters with distinct methylation signatures based on unsupervised hierarchical clustering (A). Venn diagram showing methylation changes in E-CRSwNP/ NE-CRSwNP versus control. Comparison of the differential methylation profiles associated with polyp formation among the E-CRSwNP, NE-CRSwNP, and control samples (DMCpGs). (B) Numbers of hypermethylated genes (vs. control), (C) numbers of hypomethylated genes (vs. control), (D) eosinophilic vs. non-eosinophilic tissues.

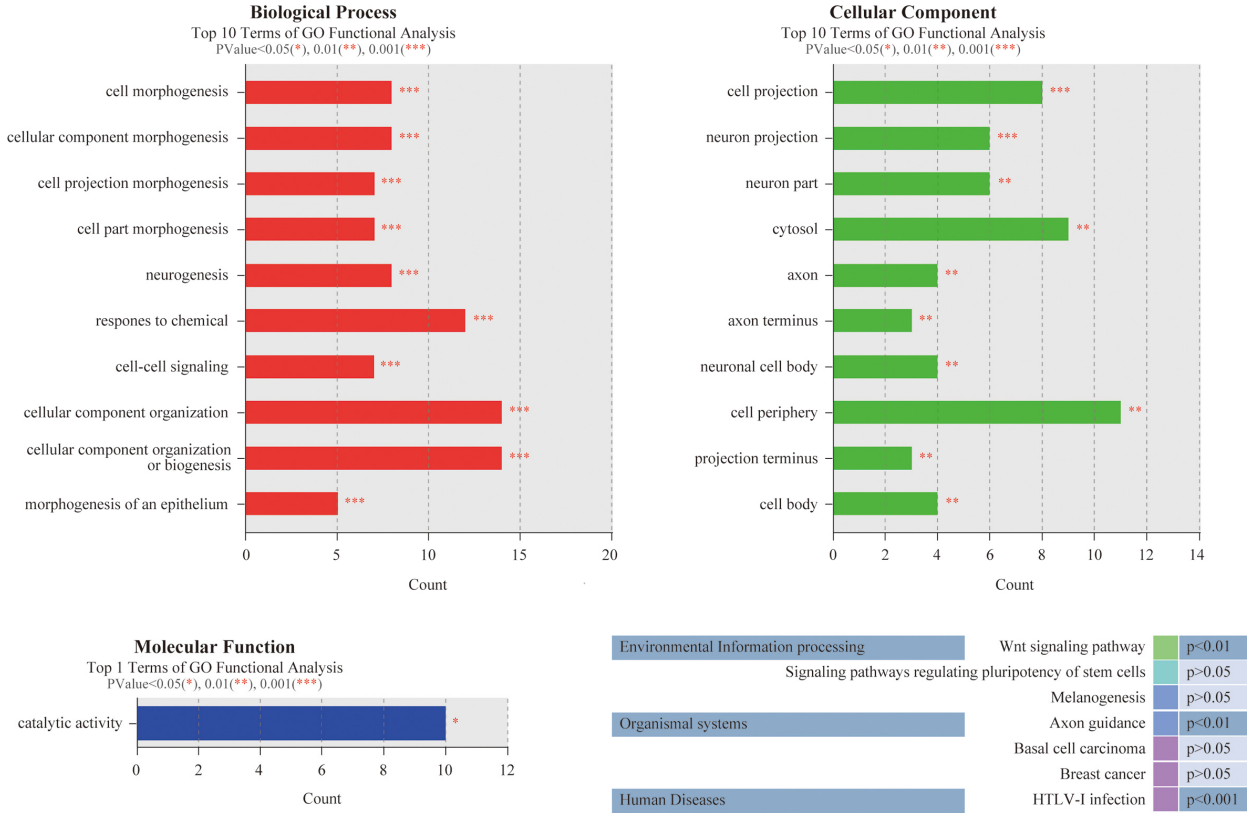

Fig. 3. DAVID functional enrichment analysis, functional Gene Ontology analysis of biological process (A), cellular component (B), molecular function (C), and KEGG enrichment analysis (D) of E-CRSwNP vs. NE-CRSwNP tissues.

Functional enrichment analysis

The methylation levels of various genomic features were found to be associated with biological processes occurring at the membrane-enclosed lumen level, especially in the E-CRSwNP tissue. In the Gene Ontology analysis, the molecular functions of most of the identified genes were associated with DNA binding, and most of the differentially methylated genes were associated with cancer pathways in the Kyoto Encyclopedia of Genes and Genomes (KEGG) pathway database. The results of the DAVID analysis are presented in Fig. 3. Differentially expressed proteins were classified according to biological processes, cellular components, and molecular functions. The functional annotation was determined for proteins showing significantly ($P < 0.05$) increased or decreased expression in the E-CRSwNP group compared with the NE-CRSwNP (Fig. 3). The results for the biological processes revealed significant differences among proteins associated with cell morphogenesis, cellular component morphogenesis, cell projection morphogenesis, cell part morphogenesis, neurogenesis, response to chemicals, cell-to-cell signaling, cellular component organization, and biogenesis and morphogenesis of epithelium (Fig. 3A). Cellular component analysis revealed significant differences among cell projection, neuron projection, neuron part, cytosol, axon, axon terminus, neuronal cell body, cell periphery, neuron projection terminus, and cell body (Fig. 3B). Findings for molecular function revealed significant differences among proteins associated with catalytic activity (Fig. 3C). The analysis of biological processes revealed significant differences among proteins associated with environmental information processing, organismal systems, and human disease (Fig. 3D).

Confirmation of gene expression using qRT-PCR

For validation of the epigenetic changes associated with eosinophil infiltration, we evaluated the mRNA expression levels of genes that have been previously reported to be closely related to E-CRSwNP (*CDH8*, *FZD5*, *PDE4B*, *WNT2*, *GSTT1*, *CCNG1*, *SLC4A8*, and *RPL17*) in samples from three patients with E-CRSwNP by qRT-PCR. The mRNA expression levels of *FZD5* and *PDE4B* were significantly increased in the samples from all three patients with E-CRSwNP compared with the NE-CRSwNP and control samples (Fig. 4A). Although the mRNA expression level of *GSTT1* was decreased in two of the patients with E-CRSwNP, the other patient showed no difference in expression between the control and NE-CRSwNP. The mRNA levels of *CDH8*, *WNT2*, *CCNG1*, *SLC4A8*, and *RPL17* did not differ significantly among the E-CRSwNP, NE-CRSwNP, and control tissues for any patient.

Protein expression in E-CRSwNP

To confirm the mRNA expression and DNA methylation data, we next conducted western blot analysis of CDH8, FZD5,

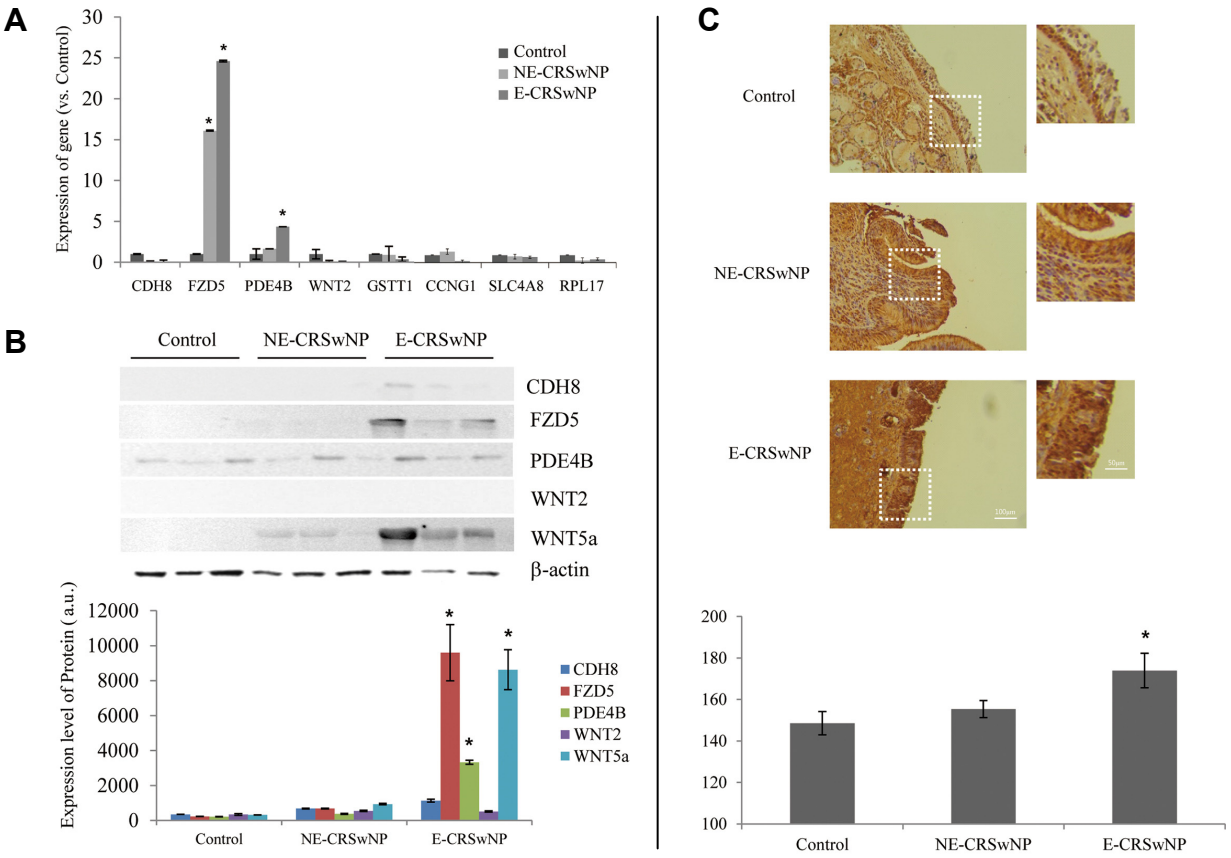

Fig. 4. (A) mRNA expression levels of *CDH8*, *FZD5*, *PDE4B*, *WNT2*, *GSTT1*, *CCNG1*, *SLC4A8*, and *RPL17* in the UP of normal mucosa and NP determined by qRT-PCR. *GAPDH* was used as the reference gene. $*P < 0.05$ vs. control. (B) Protein expression levels of CDH8, FZD5, PDE4B, WNT2, and WNT5a in the UP of normal mucosa and NP determined by western blotting. $*P < 0.05$ vs. control. FZD5 and WNT5a expression in the UP of normal mucosa and NP. (C) Immunohistochemical staining of FZD5 expression in epithelium of different sample groups. $*P < 0.001$ vs. control.

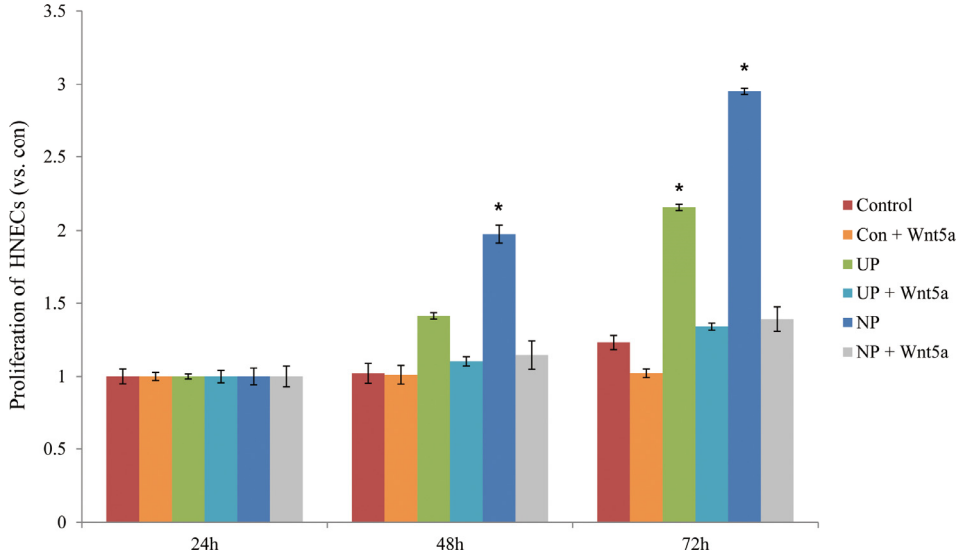

Fig. 5. Effect of FZD5 on proliferation in WNT5a-stimulated HNECs. The effect of FZD5 on HNEC proliferation was measured by MTT assay. HNECs were treated with 250 ng/mL WNT5a for 24, 48, or 72 h. Each experiment was conducted in triplicate (n = 3). $*P < 0.001$ vs. control.

PDE4B, WNT2, and WNT5a. The protein expression levels of CDH8, FZD5, PDE4B, and WNT5a were increased in E-CRSwNP samples compared with NE-CRSwNP and control samples (Fig. 4B). However, WNT2 showed no difference in expression between the patient groups.

Epithelial expression of FZD5 is higher in E-CRSwNP than in control mucosa and NE-CRSwNP

FZD5 expression in the control, NE-CRSwNP, and E-CRSwNP tissues was evaluated by histological analysis. FZD5-positive staining was mainly located in the epithelial cells and submucosal inflammatory cells. Positively stained cells were especially abundant in E-CRSwNP. The number of FZD5-positive cells was significantly higher in E-CRSwNP than in the control and NE-CRSwNP (Fig. 4C). FZD5 protein expression was significantly higher in E-CRSwNP than in control mucosa and NE-CRSwNP.

Cell proliferation is inhibited in HNECs by WNT5a stimulation

Based on the *in-vivo* observations of FZD5 expression in the nasal epithelium of CRSwNP, *in-vitro* experiments were conducted to determine whether WNT5a treatment could induce proliferation of HNECs. At a concentration of 250 ng/mL, WNT5a inhibited proliferation, without inducing cell death (Fig. 5).

Quantitative measurement of cytokines

Expression levels of various cytokines and the chemokines CCL5, CXCL10, and CXCL12 in all samples were assessed using cytokine arrays. The levels of the proinflammatory cytokines C5/C5a, CD40L, G-CSF, IL-1a, IL-10, IL-12p70, IL32a, and chemokine CXCL10 were markedly higher in the E-CRSwNP tissue samples than in the control and NE-CRSwNP tissues. Cytokine and chemokine expression levels in WNT5a-non-treated HNECs were generally very low, and no significant differences occurred in any of the measured pro-inflammatory cytokines among the E-CRSwNP, control, and NE-CRSwNP groups (Fig. 6).

DISCUSSION

In the present study, we investigated the role of eosinophils in the pathophysiology of CRSwNP in Asian subjects and the expression of FZD5 in CRS patients with or without NP. We examined the prognostic value of eosinophil and neutrophil levels in patients with bilateral NP. Patients with CRSwNP were classified based on the eosinophil/non-eosinophil ratio in NP tissue. One previous study demonstrated that WNT5 is increased in patients with E-CRSwNP compared with those

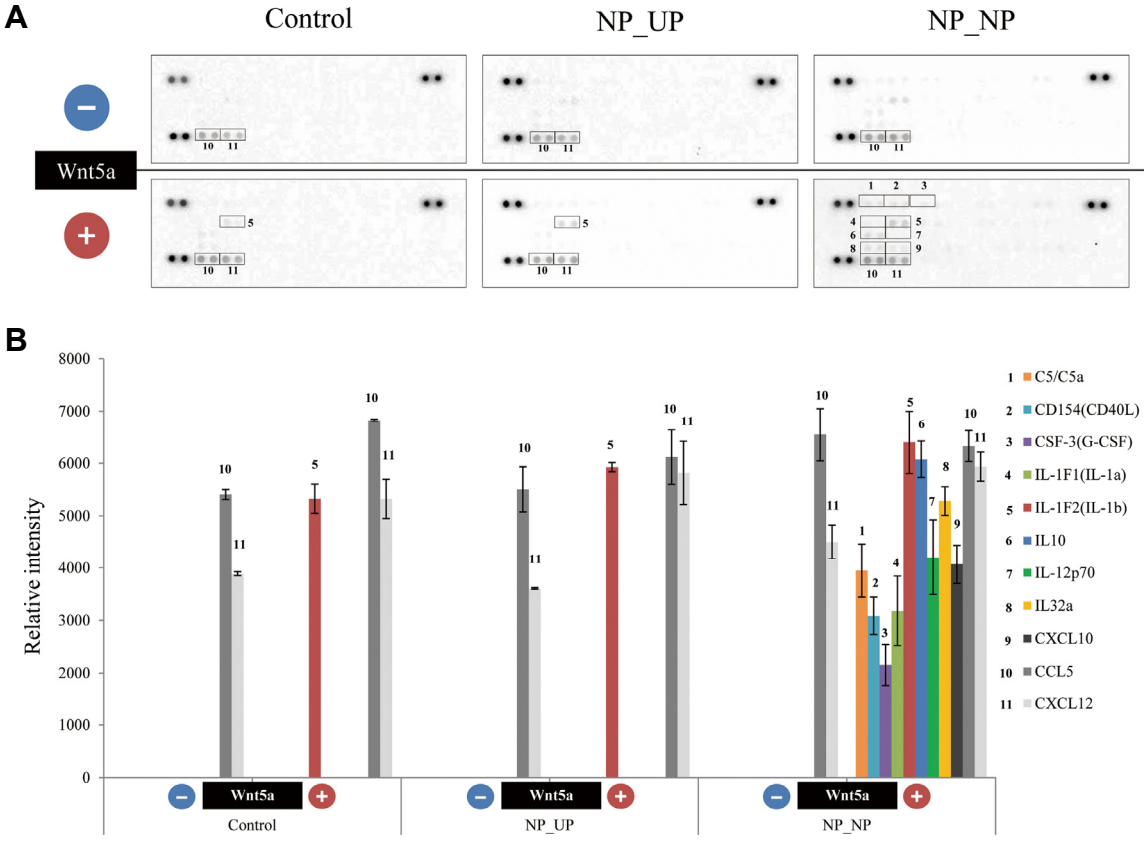

Fig. 6. Elevated levels of cytokines detected in HNECs. (A) Cytokine array (ARY005) scan showing changes in cytokine expression in WNT5a-stimulated HNECs. (B) Relative protein levels detected with the cytokine array.

with CRSwNP (Gleich and Adolphson, 1986; Wu et al., 2010). Meanwhile, FZD expression is significantly downregulated in the ethmoid mucosa of patients with CRSwNP compared with the levels in healthy controls (Kuroda et al., 2012; Slavin et al., 2005). In the current study, however, we found no significant difference in FZD5 expression in the ethmoid mucosa tissue between patients with CRSwNP and controls, but FZD5 levels were elevated in the E-CRSwNP compared with the NE-CRSwNP group.

We compared DNA methylation patterns between E-CRSwNP and NE-CRSwNP, and control tissues using MBD-seq to identify genes that are differentially methylated in E-CRSwNP. CRSwNP tissues were divided into eosinophilic and non-eosinophilic depending on whether the tissue eosinophils exceeded 10% of the total inflammatory cells. Immunohistochemistry revealed that FZD5 was mainly located in the epithelial cells in E-CRSwNP. The MBD-seq results showed that *FZD5* was significantly hypomethylated in the E-CRSwNP compared to the NE-CRSwNP group. The mRNA level of *FZD5* was higher in the E-CRSwNP than in the NE-CRSwNP group. In the normal control group, *FZD5* expression was weak. Further, the *FZD5* gene was hypomethylated in the E-CRSwNP tissues as compared with the controls.

To the best of our knowledge, this is the first report of increased FZD5 expression in patients with E-CRSwNP. Our results support the hypothesis that E-CRSwNP pathogenesis results from inflammatory changes and depends on eosinophilic, and to a lesser degree, non-eosinophilic inflammation. Furthermore, these results provide insights into the possible role of eosinophils in modifying target DNA, leading to epigenetic changes and disease development. While these results are encouraging, further studies in larger patient cohorts would be required to understand the biological significance of FZD5 in patients with E-CRSwNP.

We expected that WNT5a treatment would induce the proliferation of HNECs on the basis of a report by Bo et al. (2016). However, the experimental results were contrary to our expectations. In line with our findings, Cheng et al. (2014) reported that WNT5a suppresses colon cancer by inhibiting cell proliferation.

In conclusion, epigenetic aberrations that influence innate epithelial immunity because of activated eosinophils might play a major role in the pathogenesis of E-CRSwNP and might account for the difference in disease presentation between NE-CRSwNP and CRSsNP. Further studies are needed to define the roles of FZD5 and WNT in the pathogenesis of E-CRSwNP.

ACKNOWLEDGMENTS

We would like to thank Hwan-Woo Park for helpful discussions and technical assistance. The present study was supported by the Basic Science Research Program through the National Research Foundation of Korea, funded by the Ministry of Education, Science and Technology (grant no. 2016R1C1B2012384) and a grant of the Korea Health Technology R&D Project through the Korea Health Industry Development Institute, funded by the Ministry of Health & Welfare, Republic of Korea (grant no. HI17C2412).

REFERENCES

Fokkens, W.J., Lund, V.J., Mullol, J., Bachert, C., Alobid, I., Baroody, F., Cohen, N., Cervin, A., Douglas, R., Gevaert, P., et al. (2012). EPOS 2012: European position paper on rhinosinusitis and nasal polyps 2012. A summary for otorhinolaryngologists. Rhinology *50*, 1-12.

Hsu, J., and Peters, A.T. (2011). Pathophysiology of chronic rhinosinusitis with nasal polyp. Am. J. Rhinol. Allergy *25*, 285-90.

Hamilos, D. L. (2007). Chronic rhinosinusitis patterns of illness. Clin. Allergy Immunol. *20*, 1-13.

Sreeparvathi, A., Kalyanikuttyamma, L.K., Kumar, M., Sreekumar, N., and Veerasigamani, N. (2017). Significance of blood eosinophil count in patients with chronic rhinosinusitis with nasal polyposis. Clin. Diagn. Res. *11*, MC08-11.

Grgić, M.V., Cupić, H., Kalogjera, L., and Baudoin, T. (2015). Surgical treatment for nasal polyposis: predictors of outcome. Eur. Arch. Otorhinolaryngol. *272*, 3735-3743.

Akdis, C.A., Bachert, C., Cingi, C., Dykewicz, M.S., Hellings, P.W., Naclerio, R.M., Schleimer, R.P., and Ledford, D. (2013). Endotypes and phenotypes of chronic rhinosinusitis: a PRACTALL document of the European Academy of Allergy and Clinical Immunology and the American Academy of Allergy, Asthma & Immunology. Allergy Clin. Immunol. *131*, 1479-1490.

Payne, S.C., Borish, L., and Steinke, J.W. (2011). Genetics and phenotyping in chronic sinusitis. J. Allergy Clin. Immunol. *128*, 710-720.

Shah, S.A., Ishinaga, H., and Takeuchi, K. (2016). Pathogenesis of eosinophilic chronic rhinosinusitis. J. Inflamm. (Lond) *13*, 11.

Kim, D.K., Jin, H.R., Eun, K.M., Mutusamy, S., Cho, S.H., Oh, S., and Kim, D.W. (2015). Non-eosinophilic nasal polyps shows increased epithelial proliferation and localized disease pattern in the early stage. PLoS One *10*, e0139945.

Derycke, L., Eyerich, S., Van Crombruggen, K., Pérez-Novo, C., Holtappels, G., Deruyck, N., Gevaert, P., and Bachert, C. (2014). Mixed T helper cell signatures in chronic rhinosinusitis with and without polyps. PLoS One *9*, e97581.

Chin, D., and Harvey, R.J. (2013). Nasal polyposis: an inflammatory condition requiring effective anti-inflammatory treatment. Curr. Opin. Otolaryngol. Head Neck Surg. *21*, 23-30.

Chen, K., Yu, Z., Yang, J., and Li, H. (2018). Expression of cysteinyl leukotriene receptor GPR17 in eosinophilic and non-eosinophilic chronic rhinosinusitis with nasal polyps. Asian Pac. J. Allergy Immunol. *36*, 93-100.

Yao, S., Zhu, Y., and Chen, L. (2013). Advances in targeting cell surface signalling molecules for immune modulation. Nat. Rev. Drug. Discov. *12*, 130-146.

Ponikau, J.U., Sherris, D.A., Kephart, G.M., Kern, E.B., Gaffey, T.A., Tarara, J.E., and Kita, H. (2003). Features of airway remodeling and eosinophilic inflammation in chronic rhinosinusitis: is the histopathology similar to asthma? J. Allergy Clin. Immunol. *112*, 877-882.

Doran, E., Cai, F., Holweg, C.T.J., Wong, K., Brumm, J., and Arron, J. R. (2007). Interleukin-13 in asthma and other eosinophilic disorders. Front. Med. (Lausanne) *4*, 139.

Rothenberg, M.E., and Hogan, S.P. The eosinophil. Annu. Rev. Immunol. *24*, 147-174.

Rothenberg, M.E. (1998). Eosinophilia. N. Engl. J. Med. *338*, 1592-1600.

Rothenberg, M.E., Mishra, A., Brandt, E.B., and Hogan, S.P. (2001). Gastrointestinal eosinophils. Immunol. Rev. *179*, 139-155.

Busche, S., Shao, X., Caron, M., Kwan, T., Allum, F., Cheung, W.A., Ge, B., Westfall, S., Simon, M.M., Barrett, A., et al. (2015). Population whole-genome bisulfite sequencing across two tissues highlights the environment as the principal source of human methylome variation. Genome Biol. *16*, 290.

Lin, L., Cui, L., Zhou, W., Dufort, D., Zhang, X., Cai, C.L., Bu, L., Yang, L., Martin, J., Kemler, R., et al. (2007). β-Catenin directly regulates Islet1 expression in cardiovascular progenitors and is required for multiple aspects of cardiogenesis. Proc. Natl. Acad. Sci. USA *104*, 9313-9318.

Ueno, S., Weidinger, G., Osugi, T., Kohn, A.D., Golob, J.L., Pabon, L., Reinecke, H., Moon, R.T., and Murry, C.E. (2007). Biphasic role for Wnt/beta-catenin signaling in cardiac specification in zebrafish embryonic stem cells. Proc. Natl. Acad. Sci. USA *104*, 9685-9690.

Peterson, Y.K., Nasarre, P., Bonilla, I.V., Hilliard, E., Samples, J., Morinelli, T.A., Hill, E.G., and Klauber-DeMore, N. (2017). Frizzled-5: a high-affinity receptor for secreted frizzled-related protein-2 activation of nuclear factor of activated T-cells c3 signaling to promote angiogenesis. Angiogenesis *20*, 615-628.

Malbon, C.C. (2004). Frizzleds: new member of the superfamily of G-protein-coupled receptors. Front. Biosci. *9*, 1048-1058.

Ingham, P.W., and McMahon, A.P. (2001). Hedgehog signaling in animal development: paradigms and principles. Genes Dev. *15*, 2343-2360.

Huang, H.C., and Klein, P.S. (2004). The Frizzled family: receptors for multiple signal transduction pathways. Genome Biol. *5*, 234.

Kim, J.Y., Kim, D.K., Yu, M.S., Cha, M.J., Yu, S.L., and Kang, J. (2018). Role of epigenetics in the pathogenesis of chronic rhinosinusitis with nasal polyps. Mol. Med. Rep. *17*, 1219-1227.

North, M.L., and Ellis, A.K. (2011). The role of epigenetics in the developmental origins of allergic disease. Ann. Allergy Asthma Immunol. *106*, 355-361.

Wu, J., Kong, W., and Yu, Y. (2010). Up-regulation of Wnt5A in chronic rhinosinusitis with nasal polyps. Lin Chung Er Bi Yan Hou Tou Jing Wai Ke Za Zhi *24*, 1064-1067.

Gleich, G.J., and Adolphson, C.R. (1986). The eosinophilic leukocyte: structure and function. Adv. Immunol. *39*, 177-253.

Slavin, R.G., Spector, S.L., Bernstein, I.L., Kaliner, M.A., Kennedy, D.W., Virant, F.S., Wald, E.R., Khan, D.A., Blessing-Moore, J., Lang, D.M., et al. (2005). The diagnosis and management of sinusitis: a practice parameter update. J. Allergy Clin. Immunol. *116*, S13-S47.

Kuroda, J., Nakamura, M., Yoshida, M., Yamamoto, H., Maeda, T., Taniguchi, K., Nakazawa, N., Hatori, R., Ishio, A., Ozaki, A., et al. (2012). Canonical Wnt signaling in the visceral muscle is required for left-right asymmetric development of the Drosophila midgut. Mech. Dev. *128*, 625-639.

Bo, H., Gao, L., Chen, Y., Zhang, J., and Zhu, M. (2016). Upregulation of the expression of Wnt5a promotes the proliferation of pancreatic cancer cells *in vitro* and in a nude mouse model. 13(2),1163-1171.

Cheng, R., Sun, B., Liu, Z., Zhoa, X., Qi, L., Li, Y., and Gu, Q. (2014). Wnt5a suppresses colon cancer by inhibiting cell proliferation and epithelial-mesenchymal transition. J. Cellular Physiol. *229*, 1908-1917.